Rare Metal Materials and Engineering
Volume 48, Issue 5, May 2019
Available online at www.rmme.ac.cn

Science Press

Cite this article as: Rare Metal Materials and Engineering, 2019, 48(5): 1371-1379.

ARTICLE

Acetone-sensing Properties of $ZnFe_2O_4$ Nanofibers Prepared via Electrospinning Method

Chu Xiangfeng[1], Gan Zhengqiang[1], Bai Linshan[1], Dong Yongping[1], Marina N. Rumyantseva[2]

[1] Anhui University of Technology, Ma'anshan 243002, China; [2] Moscow State University, Moscow 119991, Russia

Abstract: Compared with zero dimensional, two dimensional and three dimensional nano-materials, one dimensional nano-materials have superior gas sensing properties. In this paper, one dimensional $ZnFe_2O_4$ nano-fibers were prepared via an electrospinning method using Zn $(NO_3)_2 \cdot 6H_2O$ and Fe $(NO_3)_3 \cdot 9H_2O$ as raw materials. The precursor was analyzed by TG-DSC, and the as-prepared samples were characterized by XRD, SEM, TEM, FTIR, nitrogen adsorption and XPS. The gas sensing properties of the as-prepared samples were investigated. The results show that $ZnFe_2O_4$ prepared at 500 ºC exhibits nano-fiber morphology. The sensor device based on $ZnFe_2O_4$ nanofibers prepared at 500 ºC exhibits excellent selectivity toward acetone at the operating temperature of 190 ºC, and the ratio of $S_{1000\ \mu L/L\ acetone}$ to $S_{1000\ \mu L/L\ ethanol}$ reaches 8. When the concentration of acetone is as low as 1 μL/L, the response is still able to reach 1.1.

Key words: nanofibers; acetone sensor; selectivity; electrospinning; $ZnFe_2O_4$

In recent years, $ZnFe_2O_4$ has drawn much attention in many research fields, such as gas sensors [1-5], humidity sensor [6], photo catalysts [7-10], magnets [11-13], Li-ion batteries [14-16] and super capacitors [17,18]. The gas sensing properties are greatly dependent on the microstructure, oxygen vacancy and the morphology of the materials, because the gas sensing reaction occurs on the surface of the gas sensing materials. The preparation method and synthesis condition parameters have an important influence on the microstructure, oxygen vacancy and the morphology of the materials. Hence, the gas sensing performances of a material reported by different research groups were different.

Zhang et al [1] prepared $ZnFe_2O_4$ tubes by pyrolysis of polyvinyl alcohol (PVA)-mediated xerogels using porous alumina as a template. The sensor based on $ZnFe_2O_4$ tubes showed lower energy consumption and higher sensitivity to organics such as ethanol and acetone than the sensor based on $ZnFe_2O_4$ nanoparticles, but the detection limits and gas sensing selectivity were not ideal. Sutka et al [2] developed a cheap, sensitive and integrated $ZnFe_2O_4$ thin film gas sensor which could detect 1 μL/L ethanol at 390 ºC with fast behavior of response and recovery, but they did not investigate the gas sensing selectivity. They fabricated a sensor based on nanosheet-assembled $ZnFe_2O_4$ hollow microspheres[3]. The sensor showed high response, excellent cycle ability and long-term stability to acetone at 215 ºC, and the detection limit for acetone reached 1 μL/L. The response ratio of $S_{100\ \mu L/L\ acetone}$ to $S_{100\ \mu L/L\ ethanol}$ was about 1.5, which means that the gas selectivity was not so good. V doping could increase the sensitivity of $ZnFe_2O_4$ nanoparticles prepared by a citrate pyrolysis method to benzene at higher operating temperatures [4]. Nano-$ZnFe_2O_4$ could also be obtained by the glycine combustion method, and the best sensor based on Nano-$ZnFe_2O_4$ showed maximum response to acetone and LPG at operating temperatures of 250 and 375 ºC, respectively.

Compared with sphere materials, one dimensional gas sensing materials show better gas sensing properties [19-22].

Received date: May 11, 2018
Foundation item: National Natural Science Foundation of China (61671019, 61271156); Research Project for University Personnel Returning from Overseas Sponsored by the Ministry of Education of China
Corresponding author: Chu Xiangfeng, Ph. D., Professor, School of Chemistry and Chemical Engineering, Anhui University of Technology, Ma'anshan 243002, P. R. China, Tel: 0086-555-2311551, E-mail: xfchu99@ahut.edu.cn

One dimensional $ZnFe_2O_4$ materials have been obtained by an electrospinning method [7,10,18,23], and they exhibited better properties. In this paper, $ZnFe_2O_4$ nano-fibers were prepared by the electrospinning method and their gas sensing properties were investigated. It was found that the sensor device based on $ZnFe_2O_4$ nanofibers prepared at 500 ºC exhibited excellent selectivity toward acetone at the operating temperature of 190 ºC, and the detection limit is as low as 1 μL/L.

1 Experiment

All of the chemical reagents used in this paper were of analytical grade. Firstly, an appropriate amount of DMF was poured into 15 mL beaker. Then, Zn $(NO_3)_2{\cdot}6H_2O$ and Fe $(NO_3)_3{\cdot}9H_2O$ were added into the solution under vigorous stirring at room temperature until the salt was dissolved completely. PVP (M_w=130 000) was then added to the mixture under stirring. Finally, the mixture changed into a yellow solution. In the solution, the mass percent of Zn $(NO_3)_2{\cdot}6H_2O$ and Fe $(NO_3)_3{\cdot}9H_2O$ was 10wt%, the mass percent of DMF was 75wt%, and the mass percent of PVP was 15wt%.

Electrospinning of the solution was carried out using a single-spinneret electrospinning setup. The solution was added into a medical syringe. The tip of the needle was connected to a high voltage, and the aluminum foil collector was ground. A potential difference of 15~18 kV was applied. The angle between the needle and the collector was about 90º. The distance between the needle and the collector was 13~15 cm. Under the action of gravity and electric field, the precursor of $ZnFe_2O_4$ can be obtained on the collector. The precursor of $ZnFe_2O_4$ nanofibers was then calcined at 200 ºC in the air atmosphere for 10 min. The temperature was then raised to 400 ºC (or 500 and 600 ºC) for 2 h. The heating rate was 1 ºC/min for all the samples. Finally, $ZnFe_2O_4$ were obtained.

The DSC-TG (Germany, Netzsch STA449F3) was used to study the formation of $ZnFe_2O_4$ at a heating rate of 5 ºC/min. The phase composition of as-prepared samples was characterized by X-ray diffraction on a Bruker D8 Advance at a scanning range of 10º~70º with Cu Kα (0.154 056 nm) radiation. The surface morphology and microstructure of samples were investigated using scanning electron microscope (Hitachi S-4800) operated at 10 kV and transmission electron microscope (Tecnai-G20) with an acceleration voltage of 200 kV. The FTIR spectra were obtained using Nicolet 6700, and the wave number range is 4000~400 cm^{-1}. The specific surface areas and the pore size distribution were estimated through the Brunauer-Emmett-Teller (BET) equation based on N_2 adsorption-desorption isotherms that were measured with a Micrometrics ASAP2010C. The chemical valence states of the elements on the surface of the samples were characterized using X-ray photoelectron spectroscopy (XPS, Thermo ESCALAB250Xi) with all binding energy corrected by contaminant carbon (E_{C1s}= 284.6 eV).

$ZnFe_2O_4$ slurry using terpineol as solvent was coated onto the surface of a prefabricated alumina tube with a small brush, and dried at 80 °C for 10 h in a vacuum oven to remove terpineol, and the thickness of the film was about 10 μm. A Ni-Cr alloy inserted into the alumina tube was used to control the operating temperature of the thick film of $ZnFe_2O_4$ in the range of 20~450 °C. The response of the sensor was defined as the ratio of the electrical resistance of gas sensor in air (R_a) to that in the test gases (R_g) when the resistances of the sensor were stable. The measurement procedures of gas sensing properties of the sensors were the same as those in our previous work [24], and the relative humidity in the base gas and the detected gases was about 50%. The response time and recovery time were defined as the time at which a sensor reaches 90% of the final signal.

2 Results and Discussion

2.1 Microstructure of $ZnFe_2O_4$

The DSC-TG curves of the precursor of $ZnFe_2O_4$ fibers are shown in Fig.1. As observed in the TG curve, the mass loss can be divided into three steps. The DSC curve showed endothermic and exothermic reactions at the corresponding temperatures. The first step occurred from room temperature to 150 ºC with a mass loss of 20% due to dehydration process and the evaporation of a part of DMF, and the DSC curve also showed a low endothermic peak (T=116.7 ºC). The second mass loss appeared between 150 and 350 ºC, which was resulted from the further evaporation of DMF and the decomposition of nitrate. The third step mass loss observed between 350 and 450 ºC could be attributed to the further evaporation of DMF and decomposition of PVP. A weak exothermic peak (T=408.1 ºC) in DSC curve corresponded to the decomposition of PVP, and a large exothermic peak (T=442.3 ºC) could also be observed, which was resulted from the formation of $ZnFe_2O_4$ crystal [1,25,26]. Based on the DSC-TG result, 450 ºC was selected as the lowest calcination temperature.

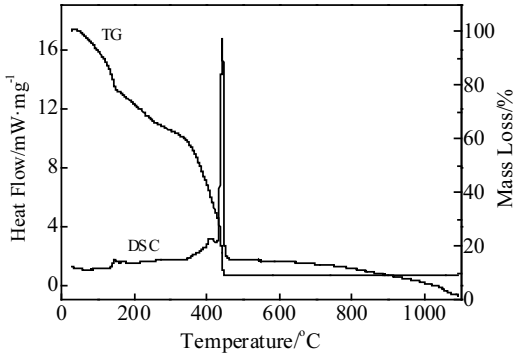

Fig.1 DSC-TG curves of the precursor of $ZnFe_2O_4$ fibers

Fig.2 shows the XRD patterns of $ZnFe_2O_4$ obtained by calcining the precursor at 450, 500, 550 and 600 ºC for 2 h. All diffraction peaks of the four samples could be well indexed to the cubic phase of $ZnFe_2O_4$ (JCPDS 79-1150) and no extra diffraction peak could be observed, which indicates that there is no impurity in the samples. The XRD peaks at 2θ values of 18.2°, 29.9°, 35.2°, 36.8°, 42.8°, 53°, 56.5°, 62.1° correspond to (111), (220), (311), (222), (400), (422), (511) and (440) crystal planes of cubic phase of $ZnFe_2O_4$, respectively. According to Scherrer's equation, the average particle sizes of $ZnFe_2O_4$ prepared at 450, 500, 550 and 600 ºC were 17, 21, 23 and 28 nm, respectively.

The SEM images of the as-prepared samples are shown in Fig.3. It was found that the morphology of the materials is less influenced by the calcination temperature. When the calcination temperature is in the range of 450~600 ºC, $ZnFe_2O_4$ nanofibers can be obtained. $ZnFe_2O_4$ nanofibers were composed of a large amount of uniform $ZnFe_2O_4$ particles with sizes around 10~40 nm, and the particle sizes observed in Fig.3 accorded with those calculated from Scherrer's equation; the diameters of $ZnFe_2O_4$ nanofibers obtained at 450, 500, 550 and 600 ºC were 160, 170, 123 and 225 nm, respectively. The diameters of nanofibers were affected by the residual carbon derived from the decomposition of PVP in the samples and the grain growth of $ZnFe_2O_4$ nanoparticles [27]. The high calcination temperature resulted in a reduction in residual carbon and grain growth, and the residual carbon and big grain size led to large diameter of nanofibers. When the calcination temperature was 550 ºC, the residual carbon was combusted completely, and the diameters of the nanofibers obtained at 550 ºC were the smallest. Fig.4 shows the TEM and HRTEM images of the sample obtained at 500 ºC. The sizes of the particles in the nanofibers and the sizes of nanofibers were also consistent with those in Fig.3; the measured *d*-spacing of 0.25 and 0.30 nm could correspond to the (311) and (220) planes of $ZnFe_2O_4$, respectively; the chemical composition of nanofiber was identified by EDX under TEM recorded from the marked area in Fig.4e, demonstrating that the nanofiber consisted mainly of Zn, Fe, O and C, and the C element signal was resulted from a little carbon decomposed from PVP; the element mappings of Zn, Fe, O exhibited homogenous spatial distributions throughout the fiber body.

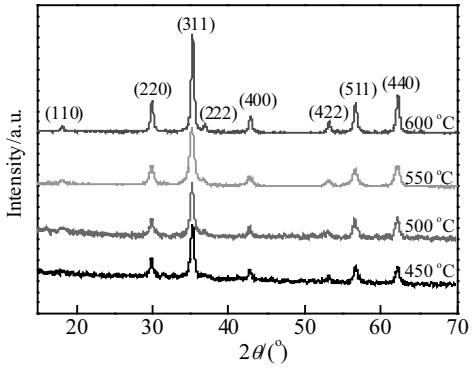

Fig.2 XRD patterns of $ZnFe_2O_4$ obtained by calcining the precursor at 450, 500, 550 and 600 ºC for 2 h

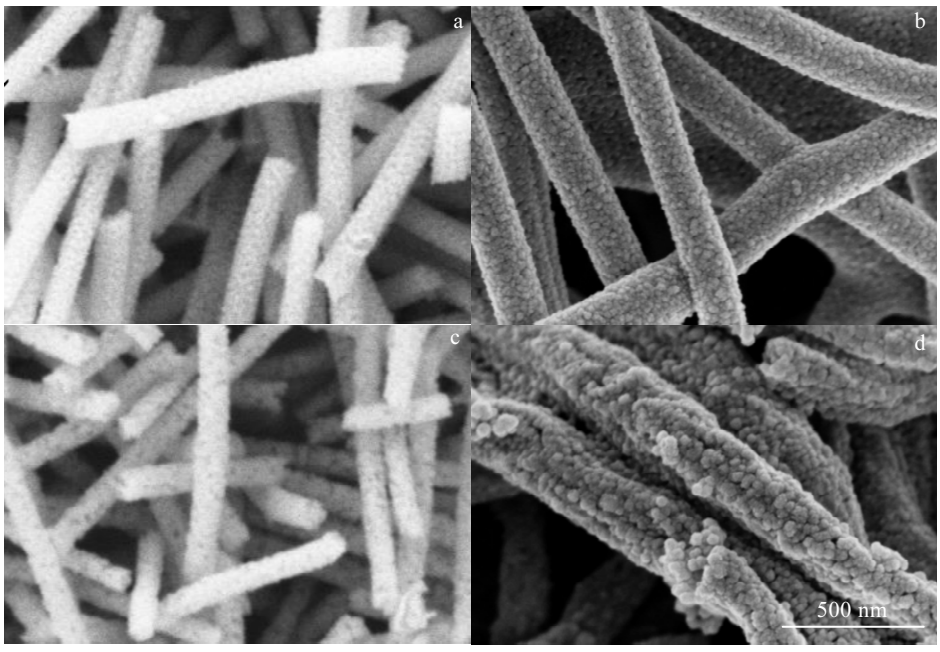

Fig.3 SEM images of the as-prepared samples obtained by calcining at 450 ºC (a), 500 ºC (b), 550 ºC (c), and 600 ºC (d)

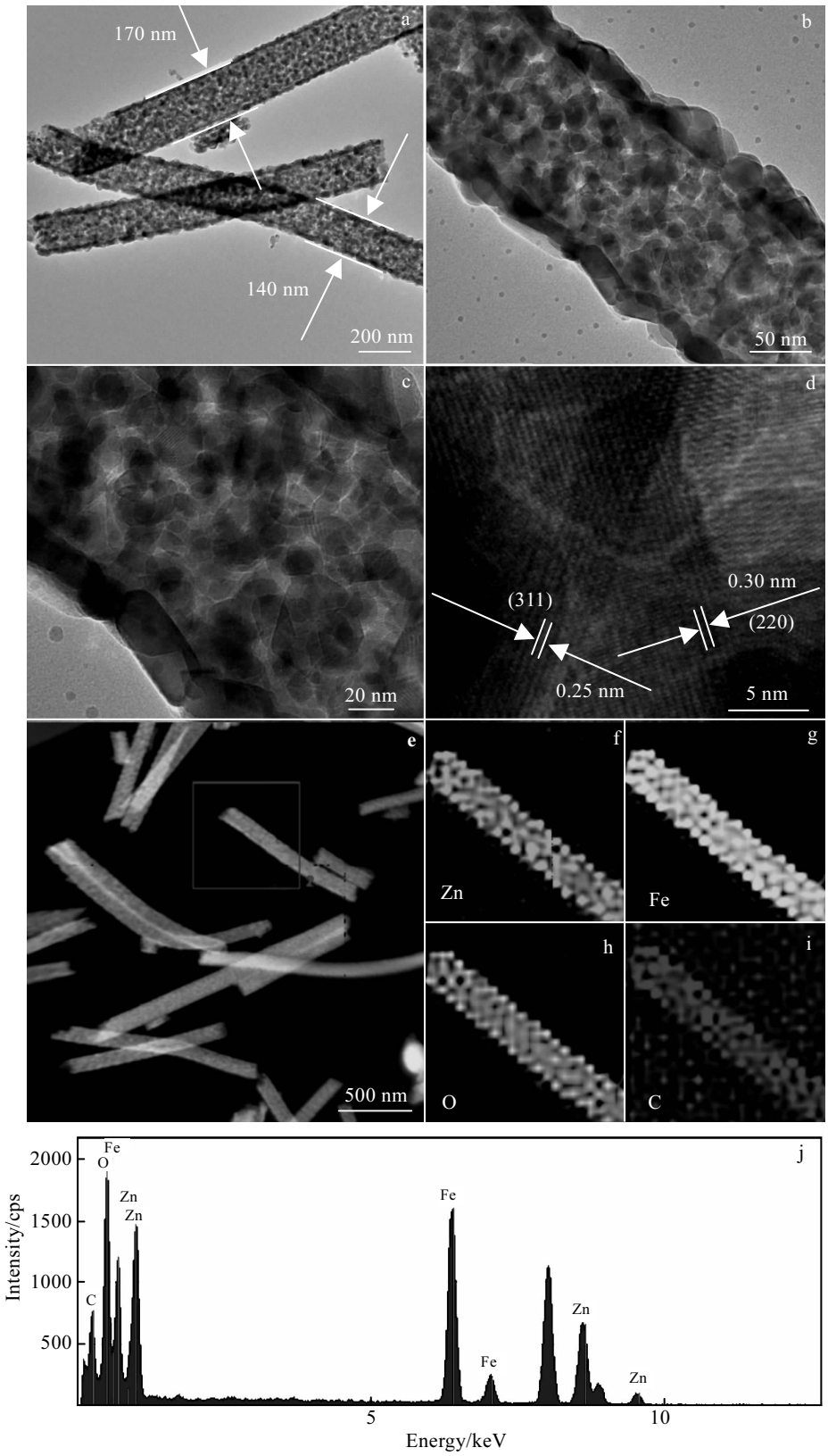

Fig.4 Typical TEM images of the as-prepared samples (500 ºC, 2 h) (a, e); HRTEM images (500 ºC, 2 h) (b, c); higher magnification HRTEM images of the marked section in Fig.4e (d); corresponding elemental mapping images (f~i) and EDS analysis (j) of individual $ZnFe_2O_4$ nanofibers marked in Fig.4e

In order to further investigate the microstructure of the material, FT-IR spectrum of $ZnFe_2O_4$ nanofibers obtained by sintering at 500 °C for 2 h in the range 4000~400 cm^{-1} is shown in Fig.5. There are several absorption peaks at 470, 568, 1390, 1600, and 3375 cm^{-1} in the spectrum. The absorption peaks appearing at 568 cm^{-1} and 470 cm^{-1} can be indexed to metal-oxygen stretching vibrations of Zn-O and Fe-O modes, respectively, which suggest the formation of $ZnFe_2O_4$ [1, 9, 28, 29]. The peak at 3375 cm^{-1} is associated with the stretching vibrations of hydrogen-bonded surface water molecules and hydroxyl groups [30]; the peak at 1600 cm^{-1} is resulted from the bending vibrations of H-O-H bands on the surface of $ZnFe_2O_4$ [31]; the weak peak at 1390 cm^{-1} might be attributed to the aliphatic C-H group vibrations of residual PVP [32].

Nitrogen adsorption-desorption measurements were used to evaluate the specific surface areas and the porosity of the as-prepared $ZnFe_2O_4$ samples. The nitrogen adsorption-desorption isotherms and pore size distribution of $ZnFe_2O_4$ obtained at 500 ºC are shown in Fig.6, and the corresponding parameters including BET surface areas and average pore sizes of all $ZnFe_2O_4$ samples are listed in Table 1. The nitrogen adsorption-desorption isotherms were close to the type of *I-V* curve [33], and the pore diameter of sample obtained at 500 ºC was around 14.77 nm, which suggests the existence of mesopores. The BET surface areas of the as-prepared samples obtained at 450, 500, 550 and 600 ºC were 19.04, 25.72, 23.36 and 21.53 $m^2 \cdot g^{-1}$, respectively. When the sintering temperature was low (450 ºC), the organic materials in the precursor did not decompose completely, and there was no enough time for the grains to grow; when the calcination temperature was higher than 500 ºC, the calcination resulted in the grain growth and high calcination temperature and then led to big crystal size and low specific surface area. The average pore sizes of the samples calcined at 450, 500, 550 and 600 ºC were 13.16, 14.77, 14.36 and 14.97 nm, respectively; these results indicate that the calcination temperature has a little influence on the average pore size.

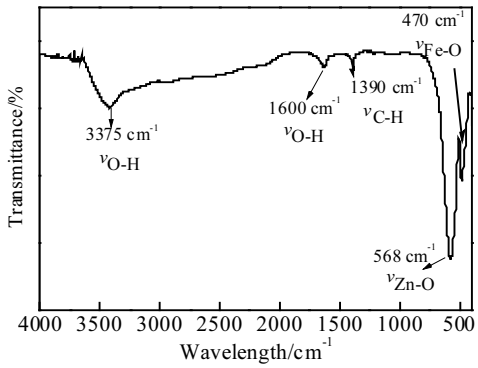

Fig.5 FTIR spectrum of $ZnFe_2O_4$ nanofiber obtained by sintering at 500 °C for 2 h in the range 4000~400 cm^{-1}

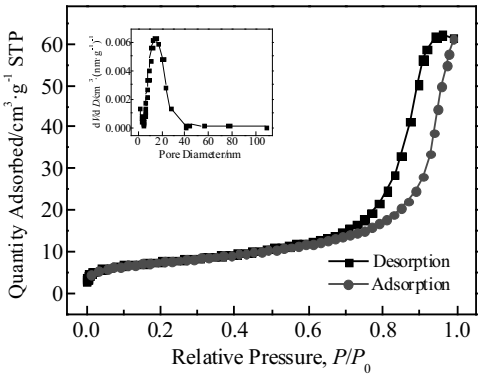

Fig.6 Nitrogen adsorption-desorption isotherms and pore size distribution of $ZnFe_2O_4$ obtained at 500 ºC

X-ray photoelectron spectroscopy was performed to characterize the composition and chemical state of the elements in $ZnFe_2O_4$ nanofibers obtained at 500 ºC, and the results are presented in Fig.7. As observed obviously in Fig.7a, the $ZnFe_2O_4$ nanofibers prepared via electrospinning are composed of Zn, Fe, O and C, which are also verified by the results of EDS analysis. Two fitted peaks centered at 1044.6 and 1021.4 eV in Fig.7b can be attributed to Zn $2p_{1/2}$ and Zn $2p_{3/2}$, respectively, [33, 34], which suggest the oxidation state of Zn^{2+} in the $ZnFe_2O_4$ nanofibers. Fig.7c depicts the XPS spectrum of Fe 2p. The peak for Fe $2p_{1/2}$ observed at 725.6 eV, and two shoulder residual peaks at 733.4 and 719.5 eV present the shakeup satellite structure [35]; the peaks for Fe $2p_{3/2}$ observed at 711.5 and 713.6 eV correspond well with the tetrahedral site (A site) and the octahedral site (B site) [33]; all the analysis about the XPS spectrum of Fe 2p suggests the Fe^{3+} oxidation state in the $ZnFe_2O_4$ nanofibers. A high-resolution peak of O 1s spectrum in Fig.7d can be resolved to two peaks with the energy of 530.3 eV for the lattice oxygen and 531.9 eV for the surface adsorbed oxygen species, and the surface absorbing oxygen species have a significant influence on the gas sensing properties of materials [35].

2.2 Gas sensing properties

Fig.8 shows the response of the sensors based on $ZnFe_2O_4$ materials obtained at 450~600 ºC for 2 h to 1000 μL/L acetone at different operating temperatures. The response of $ZnFe_2O_4$ material sintered at 450 ºC for 2 h to 1000 μL/L acetone attained the maximum values (2.0) at

Table 1 Specific surface area and pore size of $ZnFe_2O_4$ at different sintering temperatures

Temperature/ºC	450	500	550	600
BET surface area /$m^2 \cdot g^{-1}$	19.04	25.72	23.36	21.53
Pore size/nm	13.16	14.77	14.36	14.97

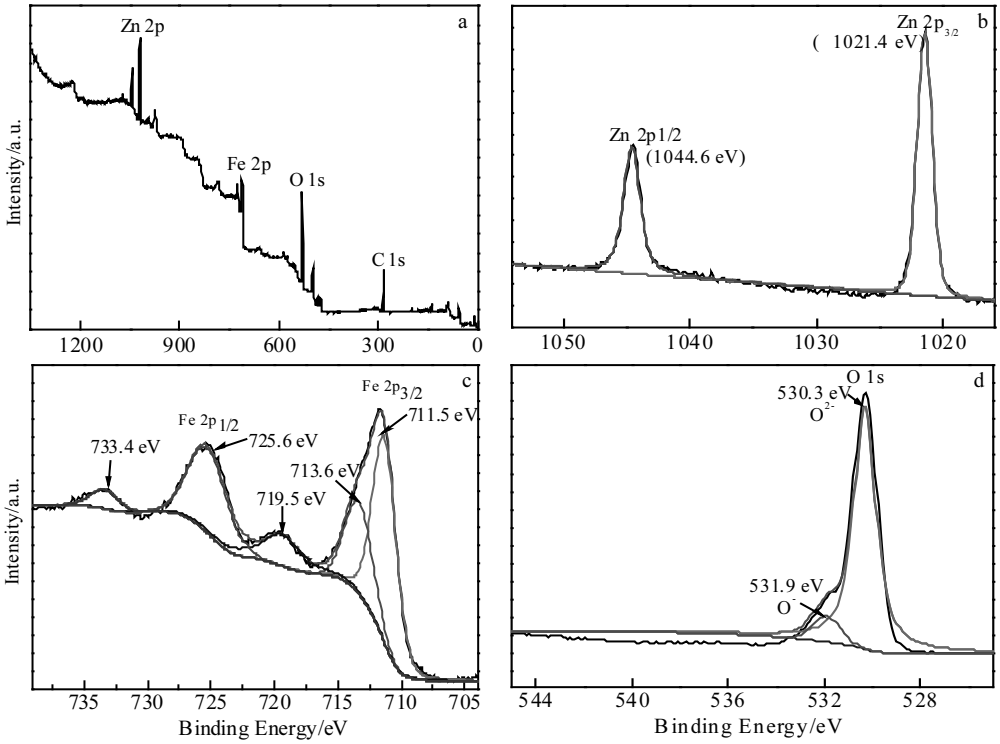

Fig.7 XPS spectra of $ZnFe_2O_4$ nanofibers obtained at 500 ºC (a), Zn 2p (b), Fe 2p (c), and O 1s (d)

Table 2 Acetone-sensing properties of $ZnFe_2O_4$ materials with different microstructures

Materials	Optimal operating temperature/ºC	Detection limit, gas sensing selectivity	Response and recovery time/s	Long-term stability/d	Ref.
Nanosheet-assembled $ZnFe_2O_4$ hollow microspheres	215	1 μL/L, $S_{acetone}/S_{ethanol}$ = 1.4	-	30	[3]
Nano-$ZnFe_2O_4$	250	100 μL/L, $S_{acetone}/S_{ethanol}$ = 2.3	120	45	[5]
$ZnFe_2O_4$ nanoparticles	200	5 μL/L, $S_{acetone}/S_{ethanol}$ = 3.5	-	-	[33]
Porous $ZnFe_2O_4$ nanorods	260	10 μL/L, $S_{acetone}/S_{ethanol}$ =3.5	<3 (10 μL/L), <10 (10 μL/L)	30	[36]
Porous $ZnFe_2O_4$ nanospheres	200	0.8 μL/L, $S_{acetone}/S_{ethanol}$ = 2	9 (30 μL/L),172 (30 μL/L)	30	[38]
$ZnFe_2O_4$ nanofibers	190	1 μL/L, $S_{acetone}/S_{ethanol}$ = 8	<15, >17	Not good	This work

Note: "-" means that there is no data in the literature

the operating temperature of 350 ºC; the maximum response (13.5) of $ZnFe_2O_4$ material sintered at 500 ºC for 2 h to 1000 μL/L acetone appeared at the operating temperature of 190 ºC; the optimal responses of the $ZnFe_2O_4$ materials sintered at 550 ºC and 600 ºC were 5.0 and 4.0, respectively. As discussed above, the large specific surface area is propitious to the adsorption of oxygen and the detected gas, and the high response of the sensor based on $ZnFe_2O_4$ materials sintered at 500 ºC for 2 h might be ascribed to its large specific surface area. The gas sensing mechanism has been investigated by many researchers[3, 33, 35-39]. The resistance variation of $ZnFe_2O_4$ sensor is resulted from the reaction between the detected gas and the chemisorbed oxygen ions on the surface of $ZnFe_2O_4$. In the air atmosphere, oxygen molecules adsorbed on the surface of $ZnFe_2O_4$ nanofibers captured electrons from conduction band of $ZnFe_2O_4$ and oxygen species ($O_2^-{}_{ads}$, $O^-{}_{ads}$, $O^{2-}{}_{ads}$) formed on the surface, which decreased electron concentration and increased the resistance of $ZnFe_2O_4$ sensor. When the sensor was exposed to an acetone atmosphere, the acetone molecules were adsorbed on the surface of $ZnFe_2O_4$, and the adsorbed acetone molecules reacted with the adsorbed oxygen. The reaction equation is as follows:

$$C_3H_6O_{ads} + 8\ O^-_{ads} = 3\ CO_2 + 3\ H_2O \quad (1)$$

This reaction process released the electrons trapped by adsorbed oxygen molecules, which decreased the resistance of $ZnFe_2O_4$ sensor in acetone atmosphere.

The gas sensing selectivity is very important for a gas sensor. The response of the sensor based on $ZnFe_2O_4$

nanofibers obtained at 500 ºC for 2 h to four kinds of gases (1000 μL/L) is shown in Fig.9. When the sensor was operated at 190 ºC, the response to 1000 μL/L acetone attained the maximum value (13.5), but the response to 1000 μL/L toluene, trimethylamine and ethanol was lower than 1.6, which means that the sensor has good selectivity to acetone; when the operating temperature was increased to 360 ºC, the response to 1000 μL/L toluene attained 5.6.

The curve of the response of the sensor $ZnFe_2O_4$ nanofibers obtained at 500 ºC for 2 h towards acetone versus acetone concentration is shown in Fig.10. When the concentration was as low as 1 μL/L, the response still reached 1.1, and the detection limit was obviously lower than that of $ZnFe_2O_4$ obtained by glycine combustion method [5]; with increasing the acetone concentration, the response increased almost linearly.

Response time and recovery time are important factors in evaluating a gas sensor. The response transient of the sensor based on $ZnFe_2O_4$ nanofibers obtained at 500 ºC to 1~1000 μL/L acetone at 190 ºC is shown in Fig.11. According to the response and recovery curves, the response time for 1000 μL/L acetone at 190 ºC was about 15 s, and the recovery time for 1000 μL/L acetone was about 17 s; when the concentration of acetone was 1 μL/L, the response time was about 7 s, and the recovery time was about 3 s, which indicates that the response and recovery time of $ZnFe_2O_4$ nanofiber sensor are both short. The response of the sensor based on $ZnFe_2O_4$ nanofibers obtained at 500 ºC for 2 h to acetone decreased a little after the sensor was placed in the air atmosphere for 10 d, and then it decreased obviously in 10~30 d, which means that the response stability is not ideal. The gas sensing instability of $ZnFe_2O_4$ nanofibers might be due to the surface contamination in air or instability of the microstructure, and the essential reason is under investigation. Table 2 lists the acetone sensing performances of $ZnFe_2O_4$ materials with different microstructures. Compared with the results reported in literatures [3, 5, 33, 38, 39], $ZnFe_2O_4$ nanofibers obtained at 500 ºC for 2 h exhibit very low response

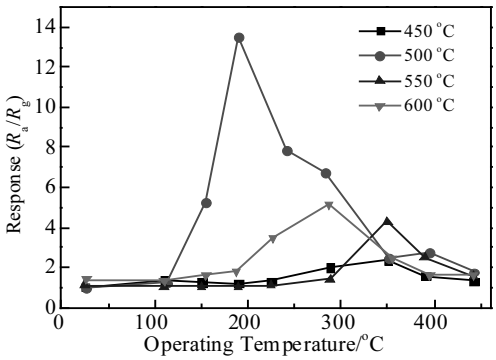

Fig.8 Response of the sensors based on $ZnFe_2O_4$ materials obtained at 450~600 ºC for 2 h to 1000 μL/L acetone at different operating temperatures

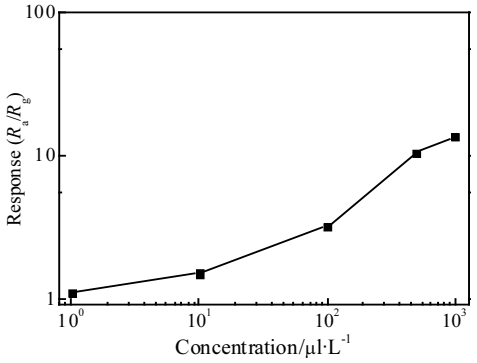

Fig.10 Response of the sensor based on $ZnFe_2O_4$ nanofibers obtained at 500 ºC for 2 h towards acetone versus acetone concentration

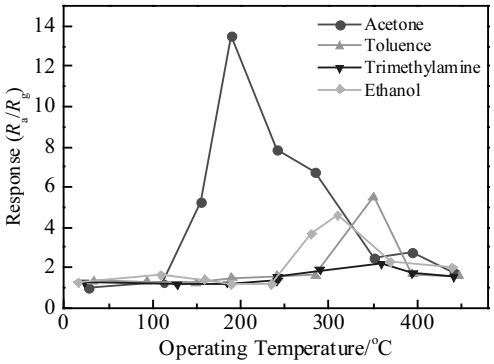

Fig.9 Response of the sensor based on $ZnFe_2O_4$ nanofibers obtained at 500 ºC for 2 h to four kinds of gases (1000 μL/L)

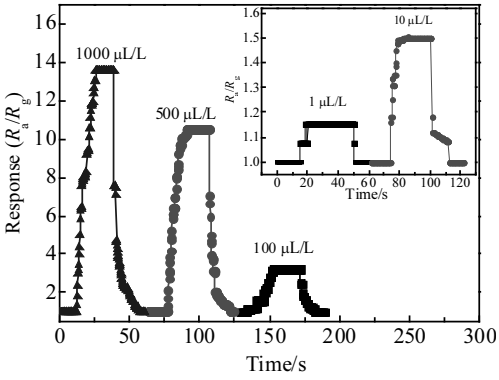

Fig.11 Response transients of the sensor based on $ZnFe_2O_4$ nanofibers obtained at 500 ºC to 1~1000 μL/L acetone at 190 ºC

to ethanol. The ratio of $S_{1000\ \mu L/L\ acetone}$ to $S_{1000\ \mu L/L\ ethanol}$ reached 8, and the gas sensing selectivity to acetone was good.

3 Conclusions

1) $ZnFe_2O_4$ nanofibers are prepared by the electrospinning method. The sensors based on $ZnFe_2O_4$ nanofibers obtained at 500 ºC for 2 h shows high response and good gas sensing selectivity to acetone when operated at 190 ºC.

2) The ratio of $S_{1000\ \mu L/L\ acetone}$ to $S_{1000\ \mu L/L\ ethanol}$ reaches 8. The detection limit can be reduced to 1 μL/L. The response time and recovery time for acetone with different concentrations are very short.

References

1 Zhang G, Li C, Cheng F *et al*. *Sensors and Actuators B Chemical*[J], 2007, 120(2): 403

2 Sutka A, Zavickis J, Mezinskis G *et al*. *Sensors and Actuators B Chemical*[J], 2013, 176(6): 330

3 Xin Z, Li X, Sun H *et al*. *Acs Applied Materials and Interfaces*[J], 2015, 7(2): 15 414

4 Jiang Y, Song W, Xie C *et al*. *Materials Letters*[J], 2006, 60(11): 1374

5 Patil J Y, Nadargi D Y, Gurav J L *et al*. *Ceramics International*[J], 2014, 40(7): 10 607

6 Tabari T, Singh D, Jamali S S. *Journal of Environmental Chemical Engineering*[J], 2017, 5(1): 931

7 Zhuo M, Yang T, Fu T *et al*. *Rsc Advances*[J], 2015, 5(84): 68 299

8 Rekhila G, Bessekhouad Y, Trari M. *Environmental Technology and Innovation*[J], 2016, 5: 127

9 Anchieta C G, Severo E C, Rigo C *et al*. *Materials Chemistry and Physics*[J], 2015, 160: 141

10 Yan J, Gao S, Wang C *et al*. *Materials Letters*[J], 2016, 184: 43

11 Guo X, Zhu H, Si M *et al*. *Journal of Physical Chemistry C*[J], 2014, 118(51): 30 145

12 Blancogutiérrez V, Torralvofernández M J, Sáezpuche R. *Journal of Physical Chemistry C*[J], 2010, 114(4): 1789

13 Zawar S, Atiq S, Riaz S *et al*. *Superlattices and Microstructures*[J], 2016, 93: 50

14 Guo X, Lu X, Fang X *et al*. *Electrochemistry Communications*[J], 2010, 12(6): 847

15 Thankachan R M, Rahman M M, Sultana I *et al*. *Journal of Power Sources*[J], 2015, 282: 462

16 Zhong X B, Yang Z Z, Wang H Y *et al*. *Journal of Power Sources*[J], 2016, 306: 718

17 Vadiyar M M, Bhise S C, Patil S K *et al*. *Rsc Advances*[J], 2015, 5(57): 45 935

18 Agyemang F O, Kim H. *Materials Science and Engineering B*[J], 2016, 211: 141

19 Xu J Q, Chen Y P, Shen J N. *Materials Letters*[J], 2008, 62(8-9): 1363

20 Lin S, Li D, Wu J *et al*. *Sensors and Actuators B Chemical*[J], 2011, 156(2): 505

21 Xiang Q, Meng G, Zhang Y *et al*. *Sensors and Actuators B Chemical*[J], 2010, 143(2): 635

22 Ding X, Zeng D, Xie C. *Sensors and Actuators B Chemical*[J], 2010, 149(2): 336

23 Wang J, Yang G, Wang L *et al*. *Electrochimica Acta*[J], 2016, 222: 1176.

24 Chu X, Chen T, Zhang W *et al*. *Sensors and Actuators B Chemical*[J], 2009, 142(1): 49

25 Yang X, Shao C, Guan H *et al*. *Inorganic Chemistry Communications*[J], 2004, 7(2):176

26 Peng C, Li G, Geng D *et al*. *Materials Research Bulletin*[J], 2012, 47(11): 3592

27 Xu M, Chang Y, Peng B *et al*. *Journal of Functional Materials*[J], 2014, 45(S2): 93 (in Chinese)

28 Masoudpanah S M, Ebrahimi S A S, Derakhshani M *et al*. *Journal of Magnetism and Magnetic Materials*[J], 2014, 370(23): 122

29 Köseoğlu Y, Baykal A, Toprak M S *et al*. *Journal of Magnetism and Magnetic Materials*[J], 2008, 462(1-2): 209

30 Wang M, Ai Z, Zhang L. *Journal of Physical Chemistry C*[J], 2008, 112(34): 13 163

31 Vinosha P A, Mely L A, Jeronsia J E *et al*. *Optik*[J], 2017, 134: 99

32 Zhang Z, Li X, Wang C *et al*. *Journal of Physical Chemistry C*[J], 2009, 113(45): 19 397

33 Zhang J, Song J M, Niu H L *et al*. *Sensors and Actuators B Chemical*[J], 2015, 221: 55

34 Wang M, Sun L, Cai J *et al*. *Journal of Materials Chemistry A*[J], 2013, 1(39): 12 082

35 Wang Y, Liu F, Yang Q *et al*. *Materials Letters*[J], 2016, 183: 378

36 Dong C, Liu X, Xiao X *et al*. *Sensors and Actuators B Chemical*[J], 2017, 239: 1231

37 Zhou X, Wang B, Sun H *et al*. *Nanoscale*[J], 2016, 8(10): 5446

38 Li L, Tan J, Dun M *et al*. *Sensors and Actuators B Chemical*[J], 2017, 248: 85

39 Zhou X, Liu J, Wang C *et al*. *Sensors and Actuators B Chemical*[J], 2015, 206: 577

静电纺丝法制备铁酸锌纳米纤维及其气敏性能研究

储向峰[1]，干正强[1]，白林山[1]，董永平[1]，Marina N. Rumyantseva[2]

(1. 安徽工业大学，安徽 马鞍山 243002)

(2. Moscow State University, Moscow 119991, Russia)

摘　要：与零维、二维和三维纳米材料相比，一维纳米材料具有优异的气敏性能。以 $Zn(NO_3)_2·6H_2O$ 和 $Fe(NO_3)_3·9H_2O$ 为原料通过静电纺丝的方法制备了一维铁酸锌纳米纤维。利用 TG-DSC 分析了材料的前驱体，用 XRD、SEM、TEM、FT-IR、BET 和 XPS 对材料进行了表征，并且对材料的气敏性能进行了研究。结果表明，在煅烧温度为 500 ℃下获得的材料呈现出纳米纤维的形貌；基于 500 ℃下获得的铁酸锌纳米纤维的元件，在工作温度为 190 ℃下对丙酮表现出较高灵敏度和高选择性，$S_{1000\ \mu L/L\ 丙酮}/S_{1000\ \mu L/L\ 乙醇}$= 8；当丙酮浓度低至 1 μL/L 时，灵敏度仍能达到 1.1。

关键词：纳米纤维；丙酮传感器；选择性；静电纺丝；铁酸锌

作者简介：储向峰，男, 1966 年生, 博士, 教授, 安徽工业大学化学与化工学院，安徽 马鞍山 243002, 电话：0555-2311551, E-mail: xfchu99@ahut.edu.cn